

Infrared optical properties of ultrathin Fe films on MgO(001) beyond the percolation threshold

G. Fahsold,* A. Bartel, O. Krauth, N. Magg, and A. Pucci

Universität Heidelberg, Kirchoff-Institut für Physik, Albert-Ueberle-Str. 3-5, 69120 Heidelberg, Germany

(Received 25 October 1999)

In ultrathin metallic films the scattering and the spatial distribution of charge are influenced by the interfaces with the vacuum and with the substrate, and by the resulting confinement of electrons. To investigate the dynamic conductivity of the free charge carriers, as the main contribution to the ir dielectric function, we used *in situ* transmission spectroscopy in the middle ir, which we performed during the evaporation of Fe on MgO(001) in ultrahigh vacuum. Up to a thickness of about 3 nm we find ir absorption and spectral dispersion clearly different from bulk iron behavior. For continuous films such findings indicate significant scattering of charge carriers at the surface and, at closer inspection of sets of spectra, a thickness dependent effective ir optical oscillator strength. The type of thickness dependence of surface scattering and of oscillator strength is correlated to the development of mesoscopic roughness during growth.

I. INTRODUCTION

The electronic properties of low-dimensional systems, e.g., of metallic thin films and nanostructures, are of basic interest for material science and a wide range of technical applications. The conductivity of metallic nanostructure defines its applicability for electronic devices.¹ This conductivity can show a modulation due to quantum size effects²⁻⁵ (QSE), which in turn can be responsible, e.g., for electron-phonon-interaction correlated growth phenomena.⁶ Furthermore, the electronic structure in low dimensional solids plays an important role in friction phenomena⁷ and it affects the surface potential,⁸ which promises a way to design catalytic properties. Finally, the interaction between adsorbates and the electronic structure of metallic low-dimensional supports gives rise to enhancement effects^{9,10} that push forward the chemical detection limit and that might be used for sensor applications.

Optical properties of conductive matter depend on electronic structure, i.e., the relaxation of electrons close to Fermi level and their optical effective mass.^{11,12} In thin films both these quantities are different from their bulk values. First, additional relaxation mechanisms due to electron-interface scattering¹³⁻¹⁵ lead to the so-called classical size effect (CSE). The CSE depends on surface roughness^{3,13,16} and it is influenced by adsorbates.¹⁷⁻²⁰ Second, the confinement of electrons due to the interfaces changes the band structure and the density of states at Fermi level.²¹⁻²³ This is the QSE. Oscillations in the optical properties^{2,24} were measured up to a thickness of several nanometers. Nevertheless, optical properties of few nanometer thick metal films on insulators are poorly investigated, which is partially due to the strong tendency of this material combination towards island growth.²⁵⁻²⁸

In this paper we report on ir-transmittance measurements of Fe/MgO(001) prepared at 315 K in ultrahigh vacuum (UHV) and their interpretation for continuous ultrathin films. The implementation of the noncontinuous island film spectra will be discussed in a forthcoming paper.²⁹ From our He-atom scattering (HAS) studies performed earlier on Fe/MgO(001),³⁰ we know that at room temperature the sub-

strate is completely covered already at a thickness of about 1 nm. This is different to many other metal-on-insulator systems.²⁵⁻²⁷ Epitaxial order was proofed by HAS and by low energy electron diffraction (LEED). At room temperature and below 0.8 nm film thickness, island growth is evidenced by HAS.³⁰ Above 1.0 nm film thickness, the continued deposition of metal reduces the roughness of the surface, i.e., the morphology that remains from the preceding island growth with grain sizes of ~ 4.0 nm^{30,31} is slowly wiped out.

Seeking for accordance between experimental ir spectra and calculations for the thin Fe films, we consider important facts: (i) the dielectric function of a metal like iron has a frequency dependence in the midinfrared (MIR) region, which is considerably different from the simple Drude model with frequency independent scattering rate and plasma frequency;³² (ii) real thin films have irregular surfaces and interfaces³⁰ that result in additional electronic relaxation and also in depolarization effects.^{27,33}

After a short description of theory (Sec. II) we give an overview of the experimental setup and present the results (Sec. III), which are analyzed with respect to thin film conductivity parameters (Sec. IV). The discussion of these parameters will illuminate their relation to the morphology of the films (Sec. V).

II. BASICS OF ir DYNAMICAL CONDUCTIVITY OF CONTINUOUS IRON FILMS

The treatment of valence electrons of a metal as a Fermi gas leads to the useful Drude-Sommerfeld approximation of the metal dielectric function as long as the energy of external excitations is too small to enable interband transitions.¹² With typical assumptions (isotropic relaxation and a phase velocity much larger than the electron velocity at Fermi energy) this dielectric function reduces to a Drude type dielectric function

$$\epsilon(\omega) = \epsilon_{\infty} - \frac{\omega_p^2}{\omega(\omega + i\omega_{\tau})}, \quad (1)$$

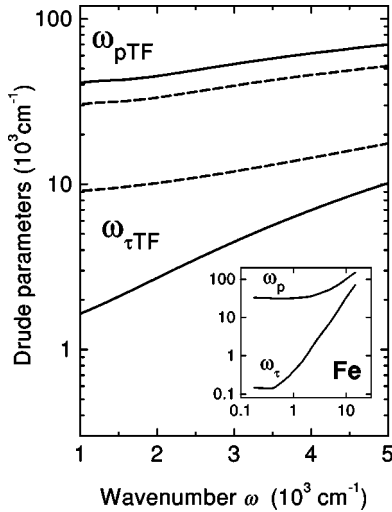


FIG. 1. Spectral behavior of the Drude parameters plasma frequency $\omega_{pTF}(\omega)$ (upper curves) and scattering rate $\omega_{\tau TF}(\omega)$ (lower curves) for iron (see text, Sec. II) found for 4.5 nm Fe/MgO(001) (solid line) and for 1.0 nm Fe/MgO(001) (dotted line). Both parameters are converted from SI units to cm^{-1} units by multiplication with $1/2\pi c$. The labels of the axes are also valid for the inset with $\omega_p(\omega)$ and $\omega_\tau(\omega)$ versus ω for bulk iron as derived from the bulk dielectric function (Ref. 32) (see text, Sec. II).

where ω is the frequency of the external field, ω_τ is the relaxation rate (i.e., the inverse life time), and ϵ_∞ accounts for the background polarizability. The optical mass m^* , which enters the plasma frequency

$$\omega_p = \sqrt{\frac{Ne^2}{\epsilon_0 m^*}}, \quad (2)$$

is an average value for the effective mass of the optical excitation process for the effective density N of the free electrons. Similar to Young's³⁴ results, frequency dependent functions have to be considered for ω_p and for ω_τ . This is the result of a renormalization procedure for effects of electron-phonon interaction in the MIR. Experimental data of various metals clearly evidence that the dielectric functions in the MIR³² are poorly described on the basis of frequency independent Drude parameters.

We derived the functions $\omega_p(\omega)$ and $\omega_\tau(\omega)$ from true frequency dependent experimental data of bulk polycrystalline iron³² by using the formal dependence of the Drude dielectric function on ω_p and on ω_τ and by setting ϵ_∞ equal to unity.³² The scattering rate calculated this way is almost frequency independent at lower frequencies, but above $\sim 2000 \text{ cm}^{-1}$ a scattering contribution that increases as ω^2 (see Fig. 1) dominates. Such contributions are also known from electron-defect scattering.³⁵ Actually, for metals at moderate temperatures they should be determined by electron-phonon scattering.³⁵

In continuous thin films the surface, the dimensionality, and the morphology influence electronic transport.^{15,27,33,36-38} With decreasing thickness of the metal film the scattering of electrons at the interfaces increasingly dominates their relaxation. This is more relevant the earlier the metal film completely covers the substrate during growth. Usually an additional relaxation rate ω_s is introduced. Ac-

cording to Matthiesen's rule, it is added to the bulk rate to give an effective thin-film relaxation rate $\omega_{\tau TF}(\omega, d)$:

$$\omega_{\tau TF}(\omega, d) = \omega_\tau(\omega) + \omega_s(d). \quad (3)$$

The surface scattering contribution $\omega_s(d)$ scales with the reciprocal average thickness d of the deposited film and with the velocity of the quasifree electrons:

$$\omega_s(d) = \alpha(d) \frac{1}{d} \frac{v_F}{2}. \quad (4)$$

We use the velocity at Fermi level¹¹ $v_F = 1.98 \times 10^6 \text{ m/s}$ and average over all directions with a positive component perpendicular to the film surface. The factor α plays a two-fold role. Originally, a probability p was used by Fuchs^{15,36} to describe the specularity of the surface scattering. For an isotropic electron gas and a film with perfectly parallel interfaces, the nonspecularity parameter α , which is proportional to $1-p$, should be equal to unity as long as each collision with an interface is counted as a scattering out of specular. In our analysis of real films the parameter α accounts for surface roughness and also for mesoscopic topography of the metallic film. A heterogeneous film thickness may be treated in a way similar to that proposed by Namba.^{15,39} By laterally averaging ω_s , i.e., the inverse film thickness, the mesoscopic roughness appears as an increase in α if the optical data are analyzed with respect to the average thickness d . The value of α may go far above unity if the mesoscopic roughness is strong. Due to this sensitivity on morphology the determination of α as a function of d supplies a tool for gaining insight into both the development of microscopic (short range, i.e., $< 1 \text{ nm}$) surface roughness and the mesoscopic (long range, i.e., $> 1 \text{ nm}$) morphology of the film.

To account for the temperature and for volume defects of the actual sample an adjustment of room temperature parameters is necessary. For example, ultrathin Fe/MgO(001) grown at room temperature shows grain boundaries^{30,31} (which may act as sources for electron scattering) at distances of typically 4 nm, which is of the same order of magnitude as the electron mean free path in polycrystalline iron in the MIR.³² For a simulation of the bulk properties of our films grown at 315 K we adjust the parameters of

$$\omega_\tau(\omega) = \omega_{\tau 0} + \gamma \omega^2, \quad (5)$$

i.e., $\omega_{\tau 0} = 860 \text{ cm}^{-1}$ and $\gamma = 3.55 \times 10^{-4} \text{ cm}^2$ for best accordance of MIR spectra of experiment and calculation for the thickest film under investigation where ω_s is small. For comparison, the data from Ref. 32 (see inset of Fig. 1) are well reproduced with $\omega_{\tau 0} = 180 \text{ cm}^{-1}$ and $\gamma = 3.20 \times 10^{-4} \text{ cm}^2$.

When calculating the thin-film dielectric function, we also take into consideration a thickness dependent variation of $\omega_p(\omega)$ and therefore replace it by $\omega_{pTF}(\omega)$:

$$\omega_{pTF}(\omega, d) = \beta(d) \omega_p(\omega). \quad (6)$$

With this scaling factor $\beta(d)$ we approximately account for QSE, for surface effects with respect to electronic polarization (from classical electrodynamics known as depolarization), and for static charge transfer.

We expect a failure of the above described model in the case of metal-island films. We also expect a less good de-

scription of experimental results for thicker (>5 nm) films and higher frequencies because in our model the scattering of electrons in the film is treated independently of the depth in the film. However, it is a good approximation as long as the film thickness d is similar or smaller than the electron mean free path $l_{MFP} = v_F / \omega_\tau$. With $v_F = 1.98 \times 10^6$ m/s this length is 5 nm at 2000 cm^{-1} , but only 1 nm at 5000 cm^{-1} for a film thickness of 4.5 nm.

If the scattering in the thin film leads to $l_{MFP} \leq \lambda_F$ ($\lambda_F = 0.37$ nm in¹¹ bulk Fe), a limit of the applicability of semi-classical calculations is reached. The onset of weak localization⁴⁰ necessitates a fully quantum mechanical treatment of the transport properties. For our continuous thin-film model we find that l_{MFP} is smaller than λ_F only for films thinner than 1 nm. Another reason for a quantum mechanical treatment is the confinement of electrons along a direction perpendicular to the surface.^{5,21,22} When $d^2 < l_{MFP} \lambda_F$ the classical picture becomes invalid and QSE should be considered.¹³ Concerning optical properties in the MIR, the transition region is again around 1 nm thickness.

III. EXPERIMENT AND RESULTS

For our experiment we used a combination of a vacuum Fourier transform ir spectrometer (Bruker IFS66v/S) with a liquid-nitrogen cooled mercury cadmium telluride (MCT) detector (Bruker) and a UHV chamber ($< 2 \times 10^{-10}$ mbar) with KBr windows and facilities for ultrathin-film preparation. A water-cooled evaporator with flux monitor (Omicron) enables Fe deposition at a controlled rate (~ 0.18 nm/min, assuming Fe bulk density). The metal vapor hits the surface at an angle of 37.5° with respect to its normal. The rate is calibrated for each experiment with a quartz microbalance (Tetra) at sample position. Average film thicknesses are derived from the deposition time. Ultraclean MgO(001) was prepared in UHV by cleavage of a $7 \times 7 \times 15 \text{ nm}^3$ sized single crystal (Kristallhandel Kelpin). The crystalline surface structure of our samples is checked with LEED (Omicron). From earlier HAS and atomic force microscopy (AFM) measurements we know that these surfaces show atomically flat terraces of several 10 nm width. We also know that cleavage in air leads to an enhanced defect density on MgO(001),^{28,41} which can alter the growth kinetics.

During thin-film deposition at room temperature ir-transmission spectroscopy was performed at a sampling rate of one spectrum (100 scans) during 0.04 nm increase of film thickness. These spectra (1800 cm^{-1} to 4500 cm^{-1}) were taken at normal incidence with a resolution of 32 cm^{-1} . As a reference, the MgO transmission is measured prior to film preparation.⁴² ir-transmission spectra for Fe films are shown in Fig. 2 for a selection of various thicknesses. Complete series of consecutively measured spectra⁴³ demonstrate that broad-band shifts in ir transmittance are well resolved down to a level of 10^{-2} nm increase of film thickness. In this experiment, we observe negative slopes for the transmittance spectra of the thinnest films. However, around 1.5 nm a crossover to positive slopes occurs. The spectra with almost no frequency dependence indicate this ir optical crossover. The transmittance decreases in the whole spectral range with increasing film thickness as demonstrated at 2000 cm^{-1} , e.g., (see Fig. 3). In the very beginning of metal deposition

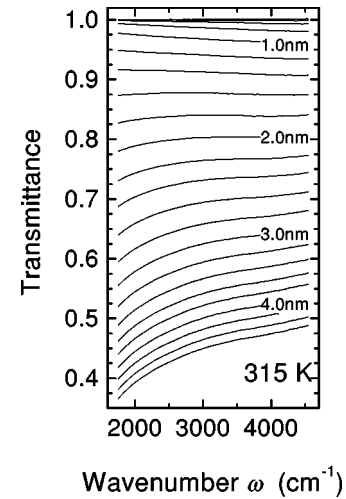


FIG. 2. Selection of transmittance spectra (normal incidence) measured for Fe growing on MgO(001) at 315 K. Unity means the same transmittance as the substrate and the labels indicate the film thickness. For successive spectra the film thickness differs by 0.2 nm.

($d < 0.8$ nm), the transmittance does not decrease remarkably, i.e., no anomalous²⁷ increase of absorption is observed. Within the experimental errors these results were reproduced several times.

IV. INTERPRETATION OF ir SPECTRA

For an interpretation of our ir optical data we calculate the ir transmittance of a layer-on-substrate system taking into account coherent multiple reflections and the continuous-thin-film model dielectric function of Sec. II. The ir transmission of the bare MgO substrate is described on the basis of the well known one-phonon parameters, the dielectric constant in the near-infrared (and visible) region, and slightly adjusted parameters of the multiphonon effects.⁴² The numerical calculations are performed with commercial software.⁴⁴

The calculated spectra of Fig. 4 are best-fit results. This

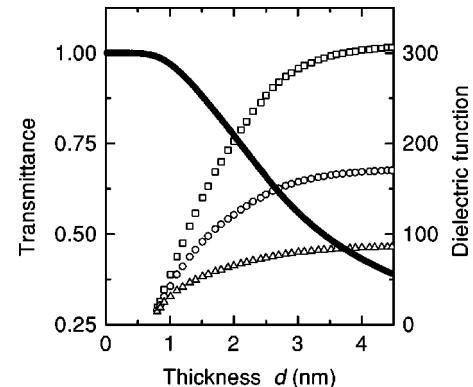


FIG. 3. Solid symbols: Transmittance at 2000 cm^{-1} versus average film thickness d for Fe growing on MgO(001) at 315 K. Open symbols: imaginary part of the Drude type continuous thin film dielectric function (see text, Sec. II) for 2000 cm^{-1} (\square), 3000 cm^{-1} (\circ), and 5000 cm^{-1} (\triangle) calculated from our fit parameters (see Fig. 5).

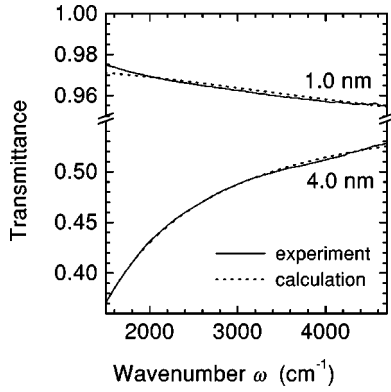


FIG. 4. Transmittance spectra for continuous Fe thin films of 1.0 nm and of 4.0 nm thickness on MgO(001). Full lines: Experimental results for growth at 315 K. Dotted line: Best fit result using frequency and thickness dependent Drude parameters (see text).

selection of spectra represents the highest accordance of measurement and calculation that could be gained in the whole thickness range from ~ 0.8 nm to 4.5 nm. We want to emphasize that the use of the frequency dependent optical parameters $\omega_p(\omega)$ and $\omega_\tau(\omega)$, which represent the actual bulk properties, is essential to gain this accordance. The only thickness dependent continuous-thin-film fit parameters are the scaling factors $\alpha(d)$ for the surface-scattering rate and $\beta(d)$ for the plasma frequency, as introduced above. Their best-fit values (see Fig. 5) are defined by a spectral mean-square fit. The importance of both these parameters is evident from the strong dependence of the mean-square deviation between experiment and calculation on the two parameters (see inset of Fig. 5). Almost no accordance is obtained if the frequency dependencies of $\omega_p(\omega)$ and $\omega_\tau(\omega)$ are ignored or if even long wave Drude parameters are used for describing the dynamic properties of iron in the MIR.³²

Coming from the highest thickness, α (and ω_s) steadily increases from a value of about 0.1 (i.e., $\omega_s = 520 \text{ cm}^{-1}$) and then it sharply increases to values far above 1.0 (i.e., 5200 cm^{-1}). At a thickness of 1.0 nm, e.g., it is 2.6 (i.e.,

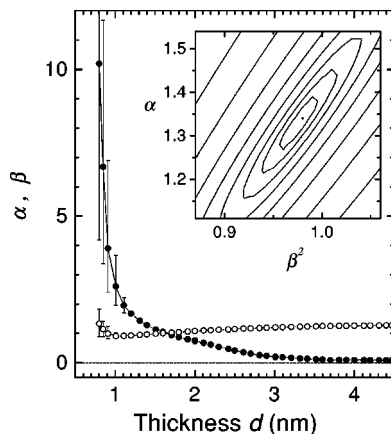


FIG. 5. Fit results for continuous thin-film parameters α (solid circles) and β (open circles) versus average film thickness d for a representative selection of our spectral data. Inset: Contour plot of the mean-square deviation of calculated spectra from experimental result for $d=1.5$ nm under variation of α and β^2 ; for successive lines the mean-square deviation changes by a factor of two.

$13\,500 \text{ cm}^{-1}$), i.e., ω_s clearly dominates in ω_{TF} . The values for β start from 1.28 at 4.5 nm, and show a gradual decay to 0.9 at 1.0 nm. Below 1.0 nm the uncertainty in the determination of the values increases (see error bars in Fig. 5) and no well-defined values can be found. This is mainly due to the fact that in the limit $\omega_s \approx \omega_{TF} \gg \omega$ the two parameters enter the dielectric function only as the ratio β^2/α .

These thickness dependencies of α and β are found for all the investigated films grown at room temperature on MgO(001) cleaved in UHV. The results are very stable with respect to small variations of the bulk properties, particularly at thicknesses below 2.0 nm. At high thicknesses, where ω_s is small, the arbitrary balance between ω_s and $\omega_{\tau 0}$ appears in the values for α [see Eqs. (3) and (4)]. We chose $\omega_{\tau 0}$ to give an $\alpha(d)$ with an approach to a constant value at 4.5 nm. The saturation behavior of β at large thickness appears reasonable. The meaning of a value above unity needs further investigations. We find values for β above unity for Fe thin films (studied up to ~ 13 nm) on several substrates and for several growth conditions. We carefully checked that it is not due to the uncertainty in the thickness calibration. Interestingly, Au film data²⁷ also indicate an increased plasma frequency at a thickness far above the percolation threshold.

V. DISCUSSION

The observed evolution of ir optical transmittance during growth of the metal thin film resembles a scheme that focuses on the percolation threshold of a metal island film.^{27,45} However, the actual reason for the behavior observed here, in particular the optical crossover at ~ 1.5 nm thickness, is different from that scheme.⁴³ For large film thicknesses (>2.0 nm), the spectral increase of ir transmittance with increasing ω is known from the simple Drude model and it is typical for metals as long as ω is sufficiently smaller than the frequency for plasma or shape resonances. For small thicknesses (<1 nm), an ir transmittance with a dispersion of opposite sign is found. Below the percolation threshold it is due to the response of separate metal particles^{27,45} as will be discussed in more detail in a forthcoming paper.²⁹ From the comparison of our ir-transmission data with detailed HAS studies^{30,43} and from dc-conductivity measurements⁴⁶ we deduce that at the optical crossover, which occurs at ~ 1.5 nm, the film already completely covers the substrate and, therefore, should be conductive. The optical crossover in this system cannot only be the result of the morphology at the critical percolation thickness.⁴⁵ It must be caused by a property of the continuous ultrathin metallic iron films.

In order to extract further information on electronic structure, percolation, and continuous-thin-film morphology we will analyze the thickness dependence of the parameters $\alpha(d)$ and $\beta(d)$. For a film with a homogeneous electronic system and parallel, but atomically rough interfaces, a non-specularity parameter α between zero and about unity is expected independent of film thickness. An increase of α points to an increase of surface roughness. At thicknesses below 2.0 nm our fit parameter α reaches values far above unity, i.e., atomic roughness seems to be topped by morphological (long range) roughness. Since the average film thickness d enters reciprocally into the scattering rate [see Eq. (4)], regions thinner than d are of stronger weight than

thicker regions. Therefore, the found behavior clearly indicates a granular morphology of the continuous Fe films on MgO(001). Such morphology is established for Fe/MgO(001) grown at room temperature by HAS³⁰ and by scanning tunneling microscopy.³¹ With further decreasing thickness, the increasing indentation between such grains should appear as a divergence in $\alpha(d)$. Our results show this divergence at $d \approx 0.8$ nm. The incomplete substrate coverage for even thinner films is corroborated by HAS experiments.³⁰ Accordingly, the thickness dependence of α indicates a percolation transition at $d \approx 0.8$ nm. The result of a film roughness that is strongly dependent on d is also derived by an interpretation of the dc conductivity that follows from our fit results in terms of a QSE model.³⁷ This model describes an increase of dc resistivity with decreasing d that is stronger than predicted by the CSE. However, also in this case the $\omega_{TF}(\omega=0, d)$ values from our experiment can only be reproduced if an increase of surface roughness with decreasing thickness is assumed. At about 1 nm film thickness, the square root of the rms fluctuations in film thickness, which is used in the QSE model³⁷ as a parameter for the film roughness, starts to exceed the film thickness. We interpret this as an indication for the percolation transition.

The decrease of the factor β with decreasing thickness is consistent with the behavior of α since it corresponds to an increase of depolarization fields. Depolarization fields become relevant whenever the local surface is tilted with respect to the electric field of the incident wave. An increase of these depolarization fields indicates an increasing amount of tilted surface area or an increasing long-range roughness amplitude. Hence, a faceted surface or a granular film seems to be an appropriate picture to explain the small values of β . Our finding is in agreement with the results of Berthier and co-workers.^{27,47} For inhomogeneous systems with conductive matter (in two or three dimensions) in an insulating matrix, they calculate a dependence of the Drude plasma frequency on the metal filling factor that shows a roughly linear increase starting from zero frequency at the percolation threshold. Considering the film above the percolation threshold as a metallic effective medium, the decrease of β with decreasing d clearly points at a percolation thickness below 1.0 nm where we find the minimum of β . The increase of β between 1.0 nm and 0.8 nm (accompanied by an increase of uncertainty) cannot be interpreted within the continuous film model. It indicates the onset of the absorption due to isolated

metal islands.^{27,47} On the basis of our thin-film model we can recognize the negative slope of the transmission spectra for $1.0 \text{ nm} < d < 1.5 \text{ nm}$ as the result of the strongly enhanced electron scattering in an ultrathin film in combination with the frequency dependence of ω_p . As soon as $\omega_{TF} \approx \omega_s \ll \omega$, the frequency dependence of the thin-film dielectric function is dominated by $\omega_p(\omega)$ [see Eq. (1)]. In this case, an increase of ω_p with ω results in a respective increase of absorption or decrease in transmission as found for a film thinner than 1.5 nm.

Combining the interpretation for $\alpha(d)$ and $\beta(d)$ we find that the ir optical crossover in Fe ultrathin films at ~ 1.5 nm is due the electronic properties of continuous metal thin films. The thickness dependencies of the parameters α and β show no significant structure at ~ 1.5 nm, but they point at a percolation threshold at ~ 0.8 nm. These findings are illustrated by the thickness dependence of the imaginary part of the dielectric function in the MIR (as calculated with the fit parameters, see Fig. 3). With decreasing thickness the monotonically decreasing values indicate a decrease of metallic absorption.

For films thinner than 0.8 nm we found no reasonable description of the experimental spectra on the basis of the continuous film model. A much better fit between calculation and experiment we reach with the model of Yamaguchi *et al.*⁴⁸ for a two-dimensional arrangement of islands.²⁹

VI. SUMMARY

Our ir-transmission study demonstrates that information on electronic structure and morphology of ultrathin films is accessible via ir optical methods. However, careful analysis of ir data and the consideration of frequency dependent optical parameters are essential. The analysis of Fe/MgO(001) shows that, e.g., the optical crossover, which we observe in the ir transmittance, is driven by electronic structure and electronic scattering but not only by the percolation transition. From our spectral ir-transmission data we deduce a granular morphology for continuous films and the percolation transition at a thickness ~ 0.8 nm.

ACKNOWLEDGMENTS

The authors gratefully acknowledge financial support by the Deutsche Forschungsgemeinschaft and the stimulating correspondence with Z. Tešanović.

*FAX: (49)6221-549262. Electronic address: fahsold@urz.uni-heidelberg.de

¹J.E. Morris, *Vacuum* **50**, 107 (1998).

²L.A. Kuzik, V.A. Yakovlev, F.A. Pudonin, and G. Mattei, *Surf. Sci.* **361/362**, 882 (1996).

³M. Jalochofski and E. Bauer, *Phys. Rev. B* **38**, 5272 (1988).

⁴M. Jalochofski, M. Hoffmann, and E. Bauer, *Phys. Rev. Lett.* **76**, 4227 (1996).

⁵G. Fischer and H. Hoffmann, *Z. Phys. B* **39**, 287 (1980).

⁶Zhenyu Zhang, Qian Niu, and Chih-Kang Shih, *Phys. Rev. Lett.* **80**, 5381 (1998).

⁷B.N.J. Persson, *Sliding Friction* (Springer, Berlin, 1998).

⁸H. Burghgraef, A.P.J. Jansen, and R.A. van Santen, *Chem. Phys.* **177**, 407 (1993).

⁹O. Krauth, G. Fahsold, N. Magg, and A. Pucci (unpublished).

¹⁰O. Krauth, G. Fahsold, and A. Lehmann, *Surf. Sci.* **433-435**, 79 (1999).

¹¹N. W. Ashcroft and N. D. Mermin, *Solid State Physics* (Holt-Saunders International Editions, New York, 1976).

¹²F. Abeles, in *Optical Properties of Solids*, edited by F. Abeles (Elsevier, Amsterdam, 1972).

¹³R. Lenk and A. Knäbchen, *J. Phys.: Condens. Matter* **5**, 6563 (1993).

¹⁴H. Ishida, *Phys. Rev. B* **52**, 10 819 (1995).

¹⁵H. Hoffmann and J. Vancea, *Thin Solid Films* **85**, 147 (1981).

¹⁶C. Hanewinkel, H. Winkes, D. Schumacher, and A. Otto, *Electrochim. Acta* **42**, 3345 (1997).

¹⁷A. Liebsch *Phys. Rev. B* **55**, 13 263 (1997).

- ¹⁸M. Hein and D. Schumacher, *J. Phys. D* **28**, 1937 (1995).
- ¹⁹K.C. Lin, R.G. Tobin, P. Dumas, C.J. Hirschmugl, and G.P. Williams, *Phys. Rev. B* **48**, 2791 (1993).
- ²⁰G. Fahsold, J. Solbrig, and A. Lehmann, *Appl. Surf. Sci.* **142**, 253 (1999).
- ²¹N. Trivedi and N.W. Ashcroft, *Phys. Rev. B* **38**, 12 298 (1988).
- ²²P. Feibelmann, *Phys. Rev. B* **27**, 1991 (1983).
- ²³J. Barnas and Y. Bruynseraede, *Solid State Commun.* **102**, 843 (1997).
- ²⁴W. Chu Huang and Juh Tzeng Lue, *Phys. Rev. B* **49**, 17 279 (1994).
- ²⁵A.K. Green, J. Dancy, and E. Bauer, *J. Vac. Sci. Technol.* **7**, 159 (1969).
- ²⁶M. Meunier and C.R. Henry, *Surf. Sci.* **307**, 514 (1994).
- ²⁷S. Berthier and J. Peiro, *J. Phys. III* **7**, 537 (1997).
- ²⁸J.B. Zhou and T. Gustafsson, *Surf. Sci.* **375**, 221 (1997).
- ²⁹P. Starzetz, G. Fahsold, and A. Pucci (private communication).
- ³⁰G. Fahsold, A. Pucci, and K.-H. Rieder, *Phys. Rev. B* **61**, 8475 (2000).
- ³¹J.F. Lawler, R. Schad, S. Jordan, and H. van Kempen, *J. Magn. Mater.* **165**, 224 (1997).
- ³²M.A. Ordal, R.J. Bell, R.W. Alexander, Jr., L.L. Long, and M.R. Querry, *Appl. Opt.* **24**, 4493 (1985).
- ³³L. Genzel and U. Kreibig, *Z. Phys. B* **37**, 93 (1980).
- ³⁴C. Young, *J. Phys. Chem. Solids* **30**, 2765 (1969).
- ³⁵J.B. Smith and H. Ehrenreich, *Phys. Rev. B* **25**, 923 (1982).
- ³⁶K. Fuchs, *Proc. Cambridge Philos. Soc.* **34**, 100 (1938).
- ³⁷Z. Tešanović, M. Jaric, and S. Maekawa, *Phys. Rev. Lett.* **57**, 2760 (1986).
- ³⁸C. Kunze, *Solid State Commun.* **87**, 359 (1993).
- ³⁹Y. Namba, *Jpn. J. Appl. Phys.* **9**, 1326 (1970).
- ⁴⁰G. Bergmann, *Phys. Rep.* **107**, 1 (1984).
- ⁴¹G. Fahsold, A. Priebe, N. Magg, and A. Pucci, *Thin Solid Films* **364**, 177 (2000).
- ⁴²N. Magg, Diploma thesis, Universität Heidelberg, 1999.
- ⁴³G. Fahsold, A. Bartel, O. Krauth, and A. Lehmann, *Surf. Sci.* **433**, 162 (1999).
- ⁴⁴SCOUT-98, software package for optical spectroscopy (Soft Science, Aachen, Germany).
- ⁴⁵C.H. Shek, G.M. Lin, J.K.L. Lai, and J.L. Li, *Thin Solid Films* **300**, 1 (1997).
- ⁴⁶C. Liu, Y. Park, and S.D. Bader, *J. Magn. Mater.* **111**, L225 (1992).
- ⁴⁷S. Berthier and K. Driss-Khodja, *Physica A* **157**, 356 (1989).
- ⁴⁸T. Yamaguchi, S. Yoshida, and A. Kinbara, *Thin Solid Films* **21**, 173 (1974).